NUKLEONIKA 2017;62(1):37–45
doi: 10.1515/nuka-2017-0006

ORIGINAL PAPER

Investigation of ^{99}Mo potential production via UO_2SO_4 liquid target irradiation in a 5 MW nuclear research reactor

Zohreh Gholamzadeh, Seyed Mohammad Mirvakili, Amin Davari, Mosoumeh Alizadeh, Atieh Joz-Vaziri

Abstract. The activation method for ^{99}Mo production in comparison to fissionable target irradiation in research reactors is less preferable. Therefore, ^{99}Mo yield using UO_2SO_4 samples was theoretically investigated. Computational results revealed admirable potential of the liquid samples for ^{99}Mo production. Low-concentrated uranyl sulphate samples could easily be handled by the irradiation box. The sample geometry optimization improves thermal hydraulic conditions and production yield. The optimized geometry including only 0.12 g ^{235}U produced 57 Ci ^{99}Mo at end-of-irradiation (EOI) with a temperature peak of 72°C during the irradiation.

Keywords: research reactor • ^{99}Mo production • uranyl sulphate • liquid target • MCNPX code

Introduction

The medical community has been weighed down by ^{99}Mo shortages due to aging of reactors such as the National Research Universal (NRU) reactor in Canada and elsewhere. There are currently no US producers of ^{99}Mo, and NRU is scheduled for shutdown in 2016, which means that another ^{99}Mo shortage is expected unless a potentially domestic ^{99}Mo producer fills the shortage.

The most routine methods of ^{99}Mo production are either by ^{98}Mo(n,γ)^{99}Mo reaction or by ^{235}U(n,f)^{99}Mo fission process; the highest specific activity of ^{99}Mo among all production methods is achieved by the second process [1, 2].

Currently, solid target plates are used for the production of ^{99}Mo. The targets are generally either miniature Al-clad fuel plates or pins containing U-Al alloy or a thin film of UO_2 coated on the inside of a stainless steel tube; these kinds of the targets have been used since 1980s [3–5]. In these targets, the separation of ^{99}Mo from the other fission products contained inside the target after irradiation is done by the target dissolution with either alkali or acid material.

However, recently some research centres have directed their attention toward liquid target application instead of the previously mentioned solid ones.

Argonne National Laboratory (ANL) is assisting two potential domestic suppliers of ^{99}Mo by examining the results of uranyl nitrate and uranyl sulphate solutions used for ^{99}Mo production. At ANL, uranyl nitrate and uranyl sulphate solutions have been irradiated at the Argonne 3 MeV Van de Graaff

Z. Gholamzadeh✉, S. M. Mirvakili, A. Davari, M. Alizadeh, A. Joz-Vaziri
Reactor Research School,
Nuclear Science and Technology Research Institute,
Tehran, Iran,
E-mail: cadmium_109@yahoo.com

Received: 30 January 2016
Accepted: 7 November 2016

Table 1. Liquid target material and dimensions modelled using MCNPX 2.6.0 code

Core specifications	Value	Unit
Fuel solution: W%: ^{235}U: 2.0412, ^{238}U: 8.2940, O: 77.0421, H: 9.4384, S: 3.1841 (185 g/l of uranium)	1.12	g/cm^3
Stainless steel cover plate: W%: Fe: 69.5, Cr: 19, Ni: 9.5, Mn: 2.0	6.50	g/cm^3
Cylindrical target dimension	4 × 15.5	cm

accelerator to study the effects of a high radiation field on solution chemistry, specifically related to pH changes, peroxide formation, and molybdenum and iodine redox chemistry. The obtained results showed the effect of a high radiation field caused by significant pH changes in uranyl nitrate solution, which resulted from the radiolysis of nitrate [6].

SHINE Medical Technologies is developing a production method that uses a deuterium-tritium (D-T) neutron generator and a noncritical aqueous solution of LEU uranyl sulphate. After 5–7 days of irradiation and 8–10 hour cooling period, the irradiated solution runs through a ^{99}Mo recovery column. The effluent is then recycled for the next irradiation. In addition, they illustrated that currently, uranyl sulphate is preferred because pH control due to generation of nitrate radiolysis products is required when irradiating nitrate solutions [7].

Also, a thesis done at Delft University investigates a variation of this production method using uranium salt dissolved in water inside an U-shaped tube located within the reactor core. This U-tube is irradiated with neutrons coming from the Hoger Onderwijs Reactor (HOR) at the Reactor Institute Delf [8].

Another work carried out at Argonne National Laboratory relied on accelerator-based production of ^{99}Mo via irradiation of uranyl sulphate solution. In the experimental work, LINAC (linear accelerator) was upgraded to 60 MeV; it operated at 35 MeV with 10 kW beam power on the target and 5-litre solution inside a stainless steel SS-304 vessel, irradiated with neutrons, which were generated through (γ,n) reaction in the tantalum target [9].

Los Alamos Laboratory reported another experimental work on a potential method of ^{99}Mo production using uranyl sulphate liquid target. The uranyl sulphate liquid samples were irradiated via a new sample delivery and retrieval capability installed at the LANSCE facility. Neutrons were produced through a bombardment of a tungsten spallation target with 800 MeV proton beam. The neutrons from the spallation target were thermalized with a graphite annulus surrounding the sample. The thermal neutron flux at the sample location was measured with bare and cadmium-covered gold foils at 1.2×10^9 n/(cm^2·s) for an average beam current of 1.3 μA [10].

To sum up, the use of uranyl salt solution presents an attractive alternative to the conventional target irradiation method of producing ^{99}Mo [11].

Obviously, after the irradiation, ^{99}Mo recovery from the liquid targets is easier and faster than routine solid LEU targets. Meanwhile, the effluent can be used for the next irradiation. Therefore, this work investigates the production potential of ^{99}Mo using uranyl sulphate liquid target irradiation in a 5 MWth nuclear research reactor.

Material and methods

In this work, general-purpose Monte Carlo N-Particle MCNPX 2.6.0 code has been used as a powerful particle transport tool with the ability to calculate steady-state reaction rates, normalization parameters, neutronic parameters, as well as fuel burnup using CINDER90 transmutation code to calculate the time-dependent parameters [12, 13].

A cylindrical stainless steel container, which is filled with uranyl sulphate solution and a 3D neutronic model, was set up using the MCNPX 2.6.0 code in cold zero power situations by means of ENDF/B-VI continuous-energy cross section. The cross sections of S(α, β) were used for the fuel solution and light water. KCODE card of the computational code was used for neutronic parameter calculations. In total, 1 500 000 particle histories were transported to decrease the calculation errors to less than 2%. The modelled liquid target specifications are presented in Table 1.

In this work, aqueous solution of UO_2SO_4 was investigated. The first chosen uranium enrichment was equal to 19.75% (^{235}U: 19.75%, ^{238}U: 80.25%) for the sulphate salt. The uranyl sulphate aqueous solution contains 0.682 M of the uranium salt, which can give a pH ~6.8.

$$UO_2SO_4 + H_2O = H_2SO_4 + UO_2$$

Fuel solution pH cannot be allowed to rise above pH 3; if it does, the precipitation of uranium and many fission products will begin. In case of sulphate solution, several 14 M H_2SO_4 drops can adjust the solution pH lower than the limitation value. However, if the pH is too low, ^{99}Mo recovery by ion exchange resin method is less effective [14].

The sulphate aqueous solution contains 185 g/l of $^{\text{enriched}}$U. A lower uranium salt concentration in the fuel solution results in a larger Kx for Mo(VI) and therefore a more effective and efficient recovery of ^{99}Mo from such solutions can be obtained [14].

The cross section view of the modelled target located inside the irradiation box of a 5 MW research reactor is depicted in Fig. 1 and Fig. 2.

The research reactor is a 5 MW-thermal (MWth) pool-type light water research reactor, which uses Al-U_3O_8 low-enriched uranium (LEU) fuel plates and provides a thermal flux on the order of 10^{13} n/(cm^2·s) in irradiation boxes.

Axial neutron flux distributions inside the irradiation box with and without the modelled

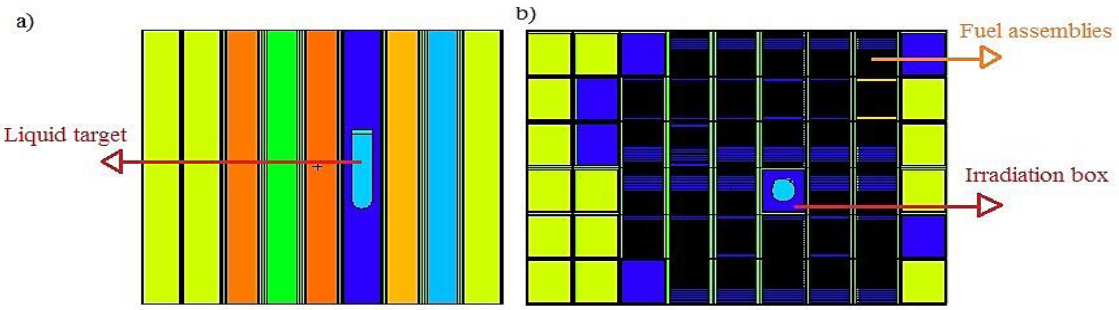

Fig. 1. Cross-sectional view of the modelled core involving the liquid target, (a) axial, (b) radial. The following colours describe: yellow – graphite blocks, blue – irradiation boxes, red – control plates and dark blue – fuel plates.

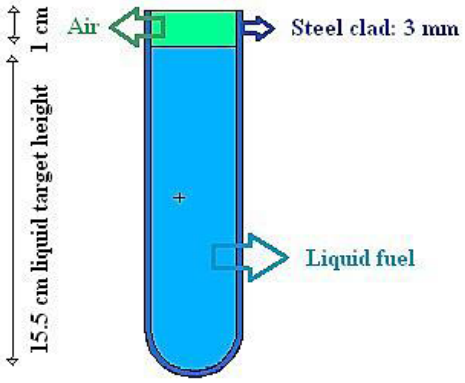

Fig. 2. Cross-sectional view of the modelled liquid target.

$^{20\%\text{- enriched}}$uranyl sulphate target containing 185 g/l of uranium were calculated using the mesh tally card of the computational code.

Different enrichments of 5, 10, 15 and 20% were considered for the uranyl sulphate solution involving 185 g/l of uranium. ^{99}Mo, ^{89}Sr and ^{131}I activities were calculated for the irradiated liquid uranyl sulphate solutions at 5 MW power, 7-day burnup + 1-day cooling. Fission per absorption ratio, radiotoxicity of the irradiated targets and total deposited heat inside the irradiated targets were calculated and discussed.

In further investigations, $^{20\%\text{ enriched}}$uranyl sulphate liquid target was selected and impact of different concentrations of dissolved uranium in the liquid targets containing 185, 92, 55 and 26 g/l values on neutronic parameters and the radioisotope production rates were discussed.

Axial-deposited power distributions were calculated using the mesh tally card for the above-mentioned liquid targets containing different concentrations of $^{20\%\text{-enriched}}$uranium. Average fission per absorption ratio was calculated using F4 tally inside the uranyl sulphate solutions. Neutron spectra available inside the solution targets as well as the irradiation box were calculated and compared with each other. The reactivity of any liquid sample positioned inside the central irradiation box was determined. Whereas void formation inside the liquid sample is probable, its effect on the core reactivity fluctuations was determined for the liquid targets containing 185, 92, 55 and 26 g/l, respectively.

Without application of any forced cooling system design in the central irradiation box, maximum concentration of uranium in the liquid target was determined to keep the peak temperature less than 100°C in natural cooling of the liquid target. The axial and radial temperature profiles were determined for the liquid target using FLUENT code. Burnup calculation of the liquid target was performed at a power of 5 MW for 7 days using the BURN card. Production rate of ^{99}Mo, ^{89}Sr, and ^{131}I radioisotopes after the burn-up time + 1-day cooling was investigated. Liquid sample geometry effects on temperature profile were discussed.

The obtained specific activity of ^{99}Mo in this work was compared with the values obtained by the other methods. Different radiochemical processes for ^{99}Mo recovery from the spent uranyl sulphate solution were reviewed.

The code uses F4 tally card to calculate neutron flux via the following equation:

$$(1)\quad \mathrm{F4} - \frac{1}{V}\int_V dV \int_E dE \int_{4\pi} d\Omega \Phi(r,E,\Omega) \left(\frac{\#}{\mathrm{cm}^2 \,/\, \text{source particle}} \right)$$

Deposited heat in the irradiated targets was calculated using F6 tally card of the used code.

The tally computes the energy deposition using Eq. (2) [13]:

$$(2)\quad \mathrm{F6} = \frac{\rho_a}{\rho_g} \int_v \int_t \int_E H(E)\Phi(r,E,t)dEdt \cdot \frac{dV}{V} \cdot \left(\frac{\mathrm{MeV}}{\mathrm{g} * (\text{source particle})} \right)$$

where ρ_a is atom density [atoms/barn-cm], ρ_g is gram density [g/cm^3] and $H(E)$ is heating response (added over nuclides in a material). F6 tally for neutrons is calculated via:

$$(3)\quad H(E) = \sigma_T(E) H_{\mathrm{ave}}(E)$$

where

$$(4)\quad H_{\mathrm{ave}}(E) = -E - \sum_i P_i(E) \left[\overline{E}_{out}(E) - Q_i + \overline{E}_{\gamma i}(E) \right]$$

and σ_T = total neutron cross section, E = incident neutron energy, $P_i(E)$ = probability of reaction i, E_{out} = average exiting neutron energy for reaction i, Q_i = Q-value of reaction i, $\overline{E}_{\gamma i}$ = average energy of exiting gammas for reaction i.

F6 tally for photons is calculated via the following equations:

$$(5)\quad H(E) = \sigma_T(E) H_{\mathrm{ave}}(E)$$

$$H_{\text{ave}}(E) = \sum_{i=1}^{3} P_i(E) * \left(E - \overline{E}_{out}\right) \quad (6)$$

where i = 1 for incoherent (Compton) scattering with form factors, i = 2 for pair production, i = 3 for photoelectric [15].

Burn card of the used code applies CINDER90 code, which originally was developed for the reactor physics community, while the code today spans applications ranging from reactor burnup over accelerator-driven transmutation to accelerator activation and to astrophysics in the evolution of elements and isotopes since the birth of the universe [16]. Mathematically, the material balance process can be described at any time by the following depletion equation:

$$\frac{dN_i}{dt} = \sum_j \gamma_{ij}\sigma_{f,j}N_j\varphi + \sum_k \sigma_{c,k\to i}N_k\varphi + \sum_l \lambda_{l\to i}N_l - \left(\sigma_{f,i}N_{ji}\varphi + \sigma_{a,i}N_{ji}\varphi + \lambda_i N_l\right) \quad (7)$$

where:
dN_i/dt = time rate of change in concentration of isotope i;
$\Sigma_j\gamma_{ij}\sigma_{f,j}N_j\varphi$ = production rate per unit volume of isotope i from fission of all fissionable nuclides;
$\Sigma_k\sigma_{c,k\to i}N_k\varphi$ = production rate per unit volume of isotope i from neutron transmutation of all isotopes including (n,γ), (n,2n), etc.;
$\Sigma_l\lambda_{l\to i}N_l$ = production rate per unit volume of isotope i from decay of all isotopes including β^-, β^+, α, γ, etc.;
$\sigma_{f,i}N_{ji}\varphi$ = removal rate per unit volume of isotope i by fission;
$\sigma_{a,i}N_{ji}\varphi$ = removal rate per unit volume of isotope i by neutron absorption (excluding fission);
$\lambda_i N_l$ = removal rate per unit of isotope i by decay [13].

Radiotoxicity of a spent fuel or irradiated liquid uranyl sulphate target could be determined by the following equation:

$$R\,[\text{Sv}] = F_d\left[\frac{\text{Sv}}{\text{Bq}}\right] \times A\,[\text{Bq}] \quad (8)$$

where F_d is dose factor and A is activity of an investigated material [17]. The liquid target radiotoxicity was determined by consideration of the following isotopes $^{239-242}$Pu, ^{237}Np, ^{129}I, ^{93}Zr, ^{135}Cs, and ^{99}Tc long half-life gamma emitter or alpha emitter isotopes available in the spent liquid target.

Results and discussion

Thermal neutron flux in order of 10^{13} n/(cm^2·s) is available inside the irradiation box of the 5 MW reactor core. Insertion of the uranyl sulphate liquid target decreases the thermal neutron flux at the sample position due to absorption of thermal neutrons by highly concentrated uranyl sulphate solution (Fig. 3).

Uranyl sulphate enrichment impacts neutronic parameters of the liquid target, and the different radioisotope production yields were investigated. Enrichment of the liquid sample containing 185 g/l of uranium was selected at 5, 10, 15 and 20%, respectively. The burn-up calculations showed that the higher enriched liquid target experiences higher fission per non-fission absorption in comparison with the 5, 10 and 15%-enriched samples. Hence, by using the higher-enriched liquid target, a nearly linear growth is observed in the production rate of the radioisotopes. In case of the $^{20\%\text{-enriched}}$uranyl sulphate, the radioisotope production yield is approximately four times higher than $^{5\%\text{-enriched}}$uranyl sulphate target. The burnt $^{20\%\text{-enriched}}$uranyl sulphate target produces about 4000 Ci of ^{99}Mo after 7 days of irradiation in a neutron flux in order of ~10^{13} n/(cm^2·s) plus 1-day cooling. After this time, ~1238 Ci of ^{131}I and 445 Ci of ^{89}Sr are produced in the irradiated solution; excluding the ^{99}Mo fission product, the produced ^{131}I and ^{89}Sr isotopes are not carrier-free, but ^{131}I would be a carrier-free product after a cooling time. Another advantage of higher-enriched liquid target application is reduction of radiotoxicity of the irradiated target. The calculations showed the higher-enriched liquid target could bear less radiotoxicity; it is related to a reduced production rate of $^{239-242}$Pu isotopes in the higher-enriched liquid target than the others (Table 2).

The radially deposited power inside the liquid $^{20\%\text{-enriched}}$uranyl sulphate target was determined using the computational code. The calculations showed peak of the deposited power is ~70 W/cm^3 in case of the liquid target bearing 185 g/l of uranium. Clearly, a reduced concentration of uranium will result in a reduced experienced power deposition by the liquid target. The 26 g/l concentration resulted in a maximum radial deposited power of 11.64 W/cm^3 inside the liquid target located in the irradiation box of the research reactor (Fig. 4). In addition, in axial direc-

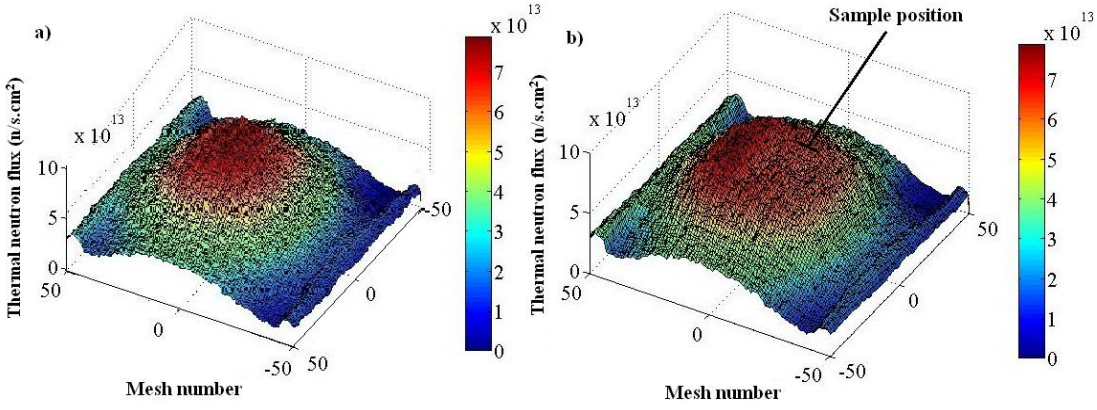

Fig. 3. Thermal neutron flux inside the irradiation box (a) in absence (b) in presence of the liquid target containing 185 g/l $^{20\%\text{-enriched}}$uranium.

Table 2. Radioisotope production rate in the different irradiated liquid targets containing 185 g/l of uranium

Solution type	^{99}Mo [Ci/g-^{235}U]	^{89}Sr [Ci/g-^{235}U]	^{131}I [Ci/g-^{235}U]	F/A ratio	Total DP [kW]	RT [Sv]
$^{5\%\text{-enriched}}$Uranyl sulphate	104.46	11.50	33.48	0.56	7.82	467
$^{10\%\text{-enriched}}$Uranyl sulphate	215.18	23.77	66.96	1.02	14.4	432
$^{15\%\text{-enriched}}$Uranyl sulphate	320.42	35.38	99.00	1.40	21.5	512
$^{20\%\text{-enriched}}$Uranyl sulphate	450.00	49.67	138.17	1.70	28.1	436

F/A: Fission per non-fission absorption ratio. DP: Deposited power. RT: Radiotoxicity.

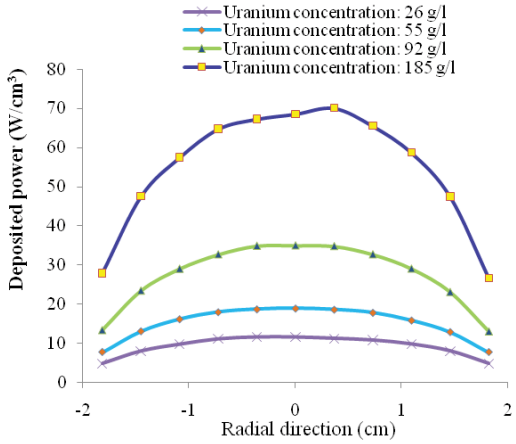

Fig. 4. Radial deposited power inside the liquid target.

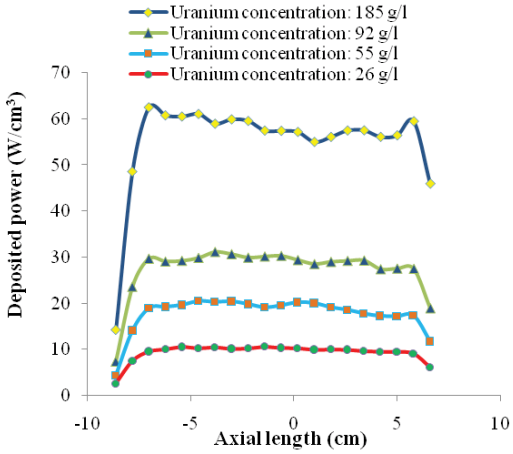

Fig. 5. Axial deposited power inside the liquid target.

tion, the liquid targets experience an approximately constant value of deposited power except upper and lower sections of the liquid targets, which obviously receive less power deposition (Fig. 5).

Different uranium concentrations were investigated for the $^{20\%\text{-enriched}}$uranyl sulphate solution. Previous calculation showed that higher-enriched liquid targets are more preferable for radiotoxicity

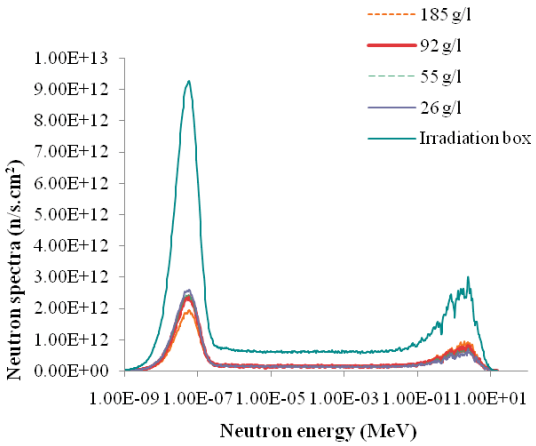

Fig. 6. Comparison of neutron spectra inside the liquid target and irradiation box.

reduction of the irradiated target and higher yield of the fission products after irradiation. As the above illustrations have shown, lower uranium concentrations could simplify the recovery of ^{99}Mo or other fission products from the irradiated solution. The calculations showed that by reduction of uranium concentration of 185 g/l to 26 g/l, the ^{99}Mo production yield decreases by a factor of 9.2. The results show that enhancement of the dissolved uranium concentration causes an exponential growth of the yield of fission products (Table 3).

The presented data in Table 3 show ^{99}Mo production yield was in range of 434–450 Ci/g-^{235}U. The different concentrations of the dissolved uranium in the uranyl sulphate solutions obtained a 47–49 Ci/g-^{235}U of ^{89}Sr after a 7-day irradiation time. ^{131}I production yield in the investigated liquid targets is on the order of 131–138 Ci/g-^{235}U.

The available spectra inside the irradiation box and liquid targets were compared with each other. As it is seen in Fig. 6, the thermal neutron flux decreased inside the liquid target because of neutron absorption by the liquid uranyl sulphate; higher uranium concentrations resulted in higher thermal neutron flux reduction. In addition, as it is seen in Fig. 7, the

Table 3. Radioisotope production rate in the different $^{20\%\text{-enriched}}$uranyl sulphate irradiated liquid targets, 7-day target irradiation at 5 MW power + 1-day cooling

Uranium concentration [g/l]	^{235}U [g]	^{99}Mo [Ci]	^{99}Mo [Ci/g-^{235}U]	^{89}Sr [Ci/g-^{235}U]	^{131}I [Ci/g-^{235}U]	F/A ratio	Total DP [kW]	RT [Sv]
185	6.806	4032	450.00	49.67	138.17	1.70	28.1	436
92	3.473	1485	427.58	47.25	131.87	1.07	12.4	231
55	2.101	913	434.55	48.07	134.22	0.50	7.85	151
26	0.986	438	444.21	49.12	136.91	0.24	3.87	65

F/A: Fission per non-fission absorption ratio. DP: Deposited power. RT: Radiotoxicity.

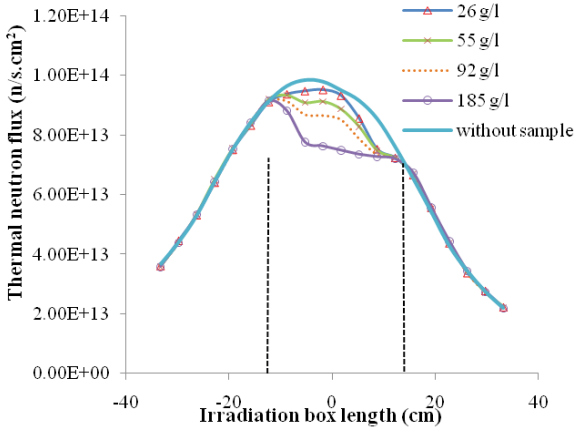

Fig. 7. Comparison of axial thermal neutron distribution inside the irradiation box with and without the uranyl sulphate liquid target.

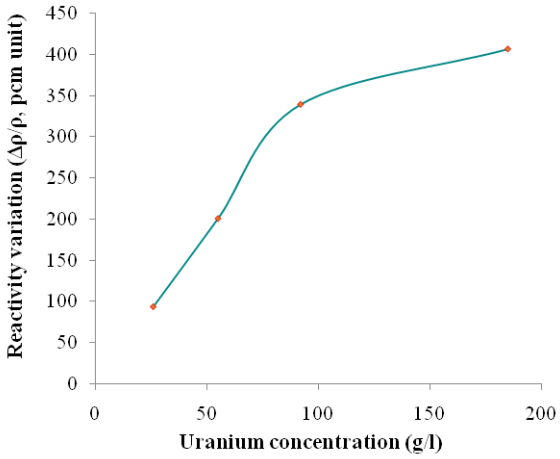

Fig. 8. Reactor core reactivity variation due to liquid target positioning inside the irradiation box.

decrease of axial thermal neutron flux is higher in case of higher concentrated uranyl sulphate target.

The modelled 5 MW research core handles up to 700 pcm of induced reactivity. Therefore, the reactor remains safe even if the transient is introduced by rapid insertion of target at its position. As Fig. 8 shows, the investigated liquid uranyl sulphate targets induce a positive reactivity of about 94 to 407 ± 32 pcm in the modelled core.

Bubble formation inside the liquid target during the 7-day irradiation is probable. Hence, its effect on effective multiplication of the research core should be determined. The computational data showed the liquid target containing higher concentrations of uranium could result in lower reactivity coefficients. However, the least concentration (26 g/l) resulted in average value of +1.5 pcm/%void reactivity coefficient, which is insignificant for the modelled research core (Fig. 9).

Whereas the liquid sample thermal conductivity is very poor in comparison with metal uranium sheets (LEU solid targets), which is used for ^{99}Mo production alternatively, maximum concentration of uranium in the liquid target was determined to keep a temperature peak of less than 100°C. Different

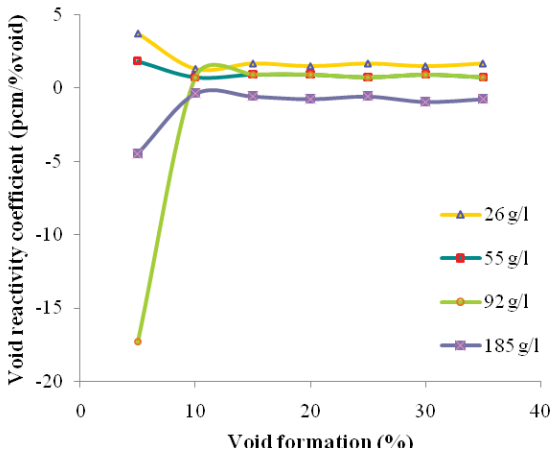

Fig. 9. Reactor void reactivity coefficient due to void formation inside the liquid target.

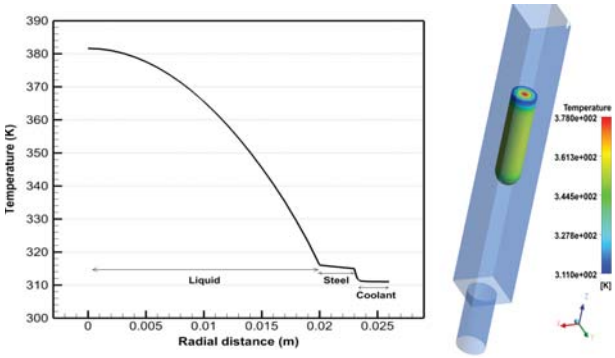

Fig. 10. The liquid target temperature profile, uranium concentration: 0.42 g/l, target dimension: 4 × 15.5 cm, coolant flow: 1 m/s.

aqueous homogeneous reactors, which operate in range of 2–2.5 W/cm^3 power density have a temperature of 70–80°C [18]. Obviously, the investigated 26–186 g/l (20.8–151 W/cm^3) concentrations need a special cooling system design to keep the temperature limit. The computational data showed a 0.42 g/l of uranium dissolved in the liquid sulphate target with 4 × 15.5 cm (diameter × height) dimension generates 300 W (1.61 W/cm^3), which is shown in its temperature profile as a peak at 110°C in the radial direction of the investigated sample. Otherwise, only 9.23 Ci of ^{99}Mo is produced in the liquid target after 7 days of irradiation (Fig. 10).

Hence, to improve thermal hydraulics of the liquid target, the area to volume ratio was increased from 1.17 to 2.34. So, seven tubes with 1.6 × 15.5 cm dimension were used instead of one tube with 4 × 15.5 cm dimension. The seven tubes contained 3.13 g/l of uranium. Any tube experiences 3.88 W/cm^3 during irradiation in the central box of the research reactor. Thermal hydraulic calculations showed that peak of temperature inside the liquid samples is 72°C. The axial and radial temperature profiles show that the seven tubes could keep temperature limit to avoid liquid sample boiling during the irradiation (Fig. 11).

Also the computational data showed the seven tubes containing uranyl sulphate solution provide 57 Ci of ^{99}Mo after 7-day burnup, which results in 12.27 six-day Ci of ^{99}Mo. The produced activity is

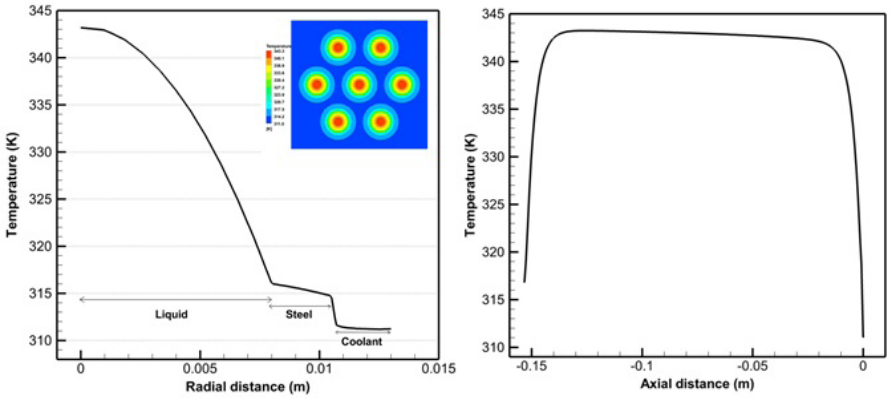

Fig. 11. The liquid target temperature profile, uranium concentration: 3.13 g/l, target dimension: 1.6 × 15.5 cm, coolant flow: 1 m/s.

457 Ci/g-^{235}U while only 0.12 g of ^{235}U existed inside the liquid samples.

As previous mentioned, ^{98}Mo(n,γ) and ^{235}U(n,f) reactor-based reactions are the most favourable ^{99}Mo production method, which could generate the highest specific activity of the product in comparison with the accelerator-based production methods. According to the literature, a production rate of 2–76 Ci/g-^{98}Mo has been reported for ^{99}Mo production via ^{98}Mo target irradiation in 14–54 MW nuclear reactors [19].

Mohammad *et al*. [20] investigated neutronic analyses and depletion calculations for the production of ^{99}Mo in Pakistan PARR-1 reactor. Analysis has been performed with 20% enriched ^{235}U plate type target (U-Al). Their calculation showed the method has the potential to produce ^{99}Mo of ~480 Ci/g-^{235}U [20].

Deuteron-induced reactions (^{98}Mo(d,p)^{99}Mo and ^{100}Mo(d,x)^{99}Mo) are another method for ^{99}Mo production. According to the obtained results by Tárkányi *et al*. [21], a typical irradiation of 8 h at 180 μA beam current on a ^{100}Mo target of 10 cm^2 area, which degrades the deuteron energy from 50 to 20 MeV, a specific activity of 4.0 Ci/g is achieved. The specific activity is comparable with the specific activity of 1.5 Ci/g for the ^{99}Mo obtained by the ^{98}Mo(n,γ) activation method at a 10^{14} n/cm^2 *s* flux in a 6-day irradiation [21].

The fission of ^{235}U provides ^{99}Mo in very high specific activity, typically greater than 5000 Ci/g [22]. The ^{98}Mo(n,γ)^{99}Mo has low specific activity, which makes it inconvenient in the extraction of ^{99m}Tc. In addition, the procedure results in additional cost in comparison with the fission of ^{235}U. However, it requires much longer time than the ^{98}Mo (n,γ)^{99}Mo for target cooling and after processing [23].

Rosental and Lewin [24] explained the ^{99}Mo production using high-current alpha beam induction on ^{96}Zr target as another new method. They demonstrated the method could produce high specific activity of ^{99}Mo (higher than 100 kCi/g).

Overview of ^{99}Mo recovery of fission products available in uranyl sulphate solution

Among different separation methods, liquid extraction could be regarded as more suitable method for recovery of ^{99}Mo from the irradiated uranium sulphate solution [25].

Alumina sorbents (Al_2O_3) are typically used for the recovery of ^{99}Mo from uranyl sulphate solutions containing LEU; however, their low capacities for Mo(VI) in concentrated uranium salt solutions is a drawback of this method [26].

A titanium oxide (TiO_2) sorbent has a higher selectivity and capacity for ^{99}Mo in concentrated uranyl sulphate LEU solutions than alumina. In addition, the adsorbed ^{99}Mo can be stripped from the sorbent using a concentrated ammonium hydroxide solution [27].

However, Mo recovery from titanium oxide is slightly easier from nitrate media compared to sulphate media. This is due to the fact that sulphate competes more strongly with molybdenum for titanium oxide adsorption sites than nitrate. In addition, a plant-scale Mo recovery column would be about 25% larger for uranyl sulphate solution compared to an uranyl nitrate solution [3].

In addition, it is reported that separation efficiency using titanium oxide sorbents can be greater than 90% at concentrations from 150 g U/l to 300 g U/l [28].

In another work done by Wu *et al*. [29], uranium solutions were prepared by dissolving uranyl nitrate in sulphuric acid solutions. The solution was irradiated in the 'Lazy Susan' facility with a thermal neutron flux of 3.4 × 10^{12} n/s·cm^2 at TRIGA reactor of the University of Illinois (USA). Recovery and purification of ^{99}Mo was carried out by its precipitation with α-benzoin oxime. The obtained results showed that 98–100% recovery yield could be obtained by a solution of 1 M H_2SO_4 and 0.5–2 M $UO_2(NO_3)_2$, using this method, in which ^{99}Mo separation via participation method was done by mixture of HNO_3, H_2SO_4, and α-benzoin oxime [29].

Conclusion

Molybdenum ^{99}Mo and other radio medical-interesting isotopes could be produced efficiently by irradiation of fissionable targets in a research reactor. This procedure is being performed by several centres using Al-UO_2 metal sheets (LEU solid targets). Some research centres have been turned their attention toward liquid uranyl sulphate or nitrate samples instead of utilizing the metal sheet.

Simpler and shorter time of ^{99}Mo recovery makes the procedure more attractive. Nevertheless, poor thermal hydraulic of the liquid targets limits the presence of higher concentrations of the dissolved uranium in the liquid sample and therefore reduces the radioisotope production yield noticeably in comparison with metal sheets of uranium, which are used in the form of LEU solid targets. Liquid sample geometry optimization could compensate for the drawback somehow. To obtain higher ^{99}Mo production yields, higher concentrations of uranium in the liquid sample are need. However, for such a sample, designing a special cooling system is required to keep the boiling temperature within the liquid target.

References

1. Rao, A., Kumar Sharma, A., Kumar, P., Charyulu, M. M., Tomar, B. S., & Rama Kumar, K. L. (2014). Studies on separation and purification of fission ^{99}Mo from neutron activated uranium aluminum alloy. *J. Appl. Radiat. Isot*., *89*, 186–191. DOI: 10.1016/j.apradiso.2014.02.013.
2. Muenze, R., Juergen Beyer, G., Ross, R., Wagner, G., Novotny, D., Franke, E., Jehangir, M., Pervez, S., & Mushtaq, A. (2013). The fission-based ^{99}Mo production process ROMOL-99 and its application to PINSTECH Islamabad. *Sci. Technol. Nucl. Install.*, *2013*, Article ID 932546, 9 pp. http://dx.doi.org/10.1155/2013/932546.
3. Ali, K. L., Ahmad Khan, A., Mushtaq, A., Imtiaz, F., MaratabZiai, A., Gulzar, A., Farooq, M., Hussain, N., Ahmed, N., Pervez, S., & Zaidi, J. H. (2013). Development of low enriched uranium target plates by thermo-mechanical processing of UAl2–Al matrix for production of ^{99}Mo in Pakistan. *J. Nucl. Eng. Des*., *255*, 77–85. DOI: 10.1016/j.nucengdes.2012.10.014.
4. Burril, K. A., & Harrison, R. J. (1989). Development of the ^{99}Mo process at CRNL. In *Fission molybdenum for medical use. Proceedings of Technical Committee Meeting organized by the International Atomic Energy Agency and held in Karlsruhe, 13–16 October 1987* (pp. 35–46). Vienna: International Atomic Energy Agency. (IAEA-TECDOC-515).
5. Arino, H., Kramer, H. H., McGovern, J. J., & Thornton, A. K. (1974). *Production of high purity fission product molybdenum-99*. U.S. Patent 3,799,883.
6. Youker, A. J., Chemerisov, S. D., Kalensky, M., Tkac, P., Bowers, D. L., & Vandegrift, G. F. (2013). A solution-based approach for Mo-99 production: Considerations for nitrate versus sulfate media. *J. Sci. Technol. Nucl. Install*., *2013*, Article ID 402570, 10 pp. http://dx.doi.org/10.1155/2013/402570.
7. Bennett, M. E., Bowers, D. L., Pereira, C., & Vandegrift, G. F. (2014). Conversion of uranyl sulfate solution to uranyl nitrate solution for processing in UREX. In 2014 Mo-99 Topical Meeting, 24–27 June 2014, Washington D.C. (S9-P1, 11 pp.). Available from http://mo99.ne.anl.gov/2014/pdfs/papers/S9P1%20Paper%20Bennett.pdf.
8. Elgin, K. (2014). *A study of the feasibility of 99Mo production inside the TU Delft Hoger Onderwijs Reactor, A Monte Carlo serpent analysis of the HOR research reactor and its medical isotope production capabilities using uranium salts*. Thesis, Delft University of Technology, The Netherlands.
9. Micklich, B. J. (2015). Remanent activation in the mini-SHINE experiments. In 3rd International Workshop on Accelerator Radiation Induced Activation (ARIA'15), 15–17 April 2015, Knoxville, Tennessee, USA (36 pp.). Available from https://public.ornl.gov/neutrons/conf/aria2015/presentations/12%20Remanent%20Activation%20in%20the%20mini-SHINE%20Experiments.pdf.
10. May, I., Rios, D., Anderson, A. S., Bitteker, L., Copping, R., Dale, G. E., Dalmas, D. A., Gallegos, M. J., Garcia, E. K., Kelsey, C. T., Mocko, M., Reilly, S. D., Stephens, F. H., Taw, F. L., & Woloshun, K. A. (2013). *A technical demonstration of the initial stage of Mo-99 recovery from a low enriched uranium sulfate solution*. Los Alamos National Laboratory. (LA-UR-13-28967).
11. Ball, R. M. (1997). Characteristics of nuclear reactors used for the production of molybdenum-99. In *Production technologies for molybdenum-99 and technetium-99m* (pp. 5–17). Vienna: International Atomic Energy Agency. (IAEA-TECDOC-1065). Availaible from http://www.iaea.org/inis/collection/NCLCollectionStore/_Public/30/013/30013597.pdf.
12. Pelowitz, D. B. (2008). *MCNPX User's Manual. Version 2.6.0.s.l.* Los Alamos National Laboratory. (LA-CP-07-1473).
13. Fensin, M. L. (2008). *Development of the MCNPX depletion capability: A Monte Carlo depletion method that automates the coupling between MCNPX and CINDER90 for high fidelity burnup calculations*. Florida University.
14. IAEA. (2008). *Homogeneous aqueous solution nuclear reactors for the production of Mo-99 and other short lived radioistotopes*. Vienna: International Atomic Energy Agency. (IAEA-TECDOC-1601).
15. Briesmeister, J. F. (2000). *MCNP-A General Monte Carlo N-Particle Transport code Version 4C*. Los Alamos National Laboratory. (LA-13709-M).
16. Gallmeier, F. X., Iverson, E. B., Lu, W., Ferguson, P. D., Holloway, S. T., Kelsey, Ch., Muhrer, G., Pitcher, E., Wohlmuther, M., & Micklich, B. (2010). The CINDER'90 transmutation code package for use in accelerator applications in combination with MCNPX. In Proceedings of the19th Meeting on Collaboration of Advanced Neutron Sources, March 8–12, 2010 (6 pp.), Grindelwald, Switzerland. Available from http://www.iaea.org/inis/collection/NCLCollectionStore/_Public/46/109/46109595.pdf?r=1.
17. Slessarev, I. (2000). *Long term radiotoxicity*. Lecture given at the Workshop on Nuclear Data and Nuclear Reactors: Physics, Design and Safety, Trieste, 13 March – 14 April, 2000 (LNS015029). Available from http://users.ictp.it/~pub_off/lectures/lns005/Number_2/Slessarev_1.pdf.
18. Rijnsdorp, S. (2014). *Design of a small Aqueous Homogeneous Reactor for production of 99Mo*. M.Sc. Thesis, Delft University of Technology, The Netherlands. Available from http://www.janleenkloosterman.nl/reports/thesis_rijnsdorp_2014.pdf.
19. Köster, U. (2011). *Present day production of ^{99}Mo and alternatives*. Grenoble: Institut Laue Langevin.
20. Mohammad, A., Mahmood, T., & Iqbal, M. (2009). Fission MOLY production at PARR-1 using LEU plate type target. *J. Nucl. Eng. Des*., *239*, 521–525. DOI: 10.1016/j.nucengdes.2008.11.008.
21. Tárkányi, F., Hermanne, A., Takács, S., Sonck, M., Szücs, Z., Király, B., & Ignatyuk, A. V. (2011). Investigation of alternative production routes of ^{99m}Tc: deuteron induced reactions on ^{100}Mo. *J. Appl. Radiat. Isot*., *69*, 18–25. DOI: 10.1016/j.apradiso.2010.08.006.

22. Ruth, T. J. (2015). *The medical isotope crisis: How we got here and where we are going*. Vancouver, British Columbia, Canada: TRIUMF and the British Columbia Cancer Agency.
23. Jun, B. J., Tanimoto, M., Kimura, A., Hori, N., Izumo, H., & Tsuchia, K. (2010). *Feasibility study on mass production of (n,γ)^{99}Mo*. Japan Atomic Energy Agency. (JAEA-Research 2010-046).
24. Rosenthal, G. B., & Lewin, H. C. (2014). Production of 99Mo using high-current alpha beams. In NNSA's 2014 Mo-99 Topical Meeting, 24–27 June 2014, Washington D.C. Available from http://mo99.ne.anl.gov/2014/pdfs/papers/S11P4%20Paper%20Rosenthal.pdf.
25. Faghihian, H., Malekpour, A., & Maragheh, M. G. (2003). Modification of clinoptilolite by surfactants for molibdate (99Mo) adsorption from aqueous solutions. *J. Sci. Islamic Republic of Iran*, *14*, 239–245.
26. Stepinski, D. C., Gelis, A. V., Gentner, P., Bakel, A., & Vandegrift, G. F. (2008). Evaluation of Radsorb, Isosorb (Termoxid) and PZC as potential sorbents for separation of ^{99}Mo from a homogeneous-reactor fuel solution. In *Homogeneous aqueous solution nuclear reactor for the production of Mo-99 and other short lived radioisotopes* (pp. 73–80). Vienna: International Atomic Energy Agency. (IAEA-TECDOC-1601). Available from http://www-pub.iaea.org/MTCD/Publications/PDF/te_1601_web.pdf.
27. Ling, L., Chung, P. L., Youker, A., Stepinski, D. C., Vandegrift, G. F., & Wang, N. H. L. (2013). Capture chromatography for Mo-99 recovery from uranyl sulfate solutions: Minimum-column-volume design method. *J. Chromatogr. A*, *1309*, 1–14. DOI: 10.1016/j.chroma.2013.08.023.
28. Dale, G. E., Dalmas, D. A., Gallegos, M. J., Jackman, K. R., Kelsey, C. T., May, I., Reilly, S. D., & Stange, G. M. (2012). 99Mo separation from high-concentration irradiated uranium nitrate and uranium sulfate solutions. *J. Ind. Eng. Chem. Res*., *51*, 13319–13322. DOI: 10.1021/ie3008743.
29. Wu, D., Landsberger, S., Buchholz, B. A., & Vandegrift, G. F. (1994). *Processing of LEU targets for ^{99}Mo production – testing and modification of the cintichem process*. Lecture presented at the 1995 International Meeting on Reduced Enrichment for Research and Test Reactors, September 18–21,1994, Paris, France. Available from http://www.rertr.anl.gov/MO99/WU95.pdf.